Journal of Inorganic and General Chemistry
ZAAC
Zeitschrift für anorganische und allgemeine Chemie
www.zaac.wiley-vch.de
RESEARCH ARTICLE
DOI: 10.1002/zaac.202200332

Na_7RbTl_4 – A New Ternary *Zintl* Phase Containing $[Tl_4]^{8-}$ Tetrahedra

Vanessa F. Schwinghammer,[a] Melissa Janesch,[a] Nikolaus Korber,[a] and Stefanie Gärtner*[a, b]

Dedicated to the late Professor Rudolf Hoppe on the occasion of his 100th birthday.

Na_7RbTl_4 has been prepared by solid state reaction from the elements. Single crystal X-ray structure analysis suggested the presence of pseudo-merohedral twinning. The final model could be derived in space group *Pbam* (a = 16.3584(4) Å, b = 16.3581(4) Å, c = 11.3345(3) Å, V = 3033.04(14) Å^3, R_1/wR_2 0.0282/0.0402) and proved the presence of isolated $[Tl_4]^{8-}$ anions, which are only known from two other solid state thallide phases so far. The structure of Na_7RbTl_4 is compared to the long-known Na_2Tl and the similarities and differences in the three-dimensional arrangement within the crystal structures are reported on. DOS calculations revealed a pseudo-band gap at E_F. Dissolution experiments in the style of the chemistry of group 14 and group 15 Zintl anions in liquid ammonia yielded degradation of the thallides. Subsequent characterization of the reaction products by powder X-ray diffraction allowed for the determination of alkali metal amide and elemental thallium as products.

Introduction

The observations of a green solution during the reaction of sodium and elemental lead in liquid ammonia by *Joannis* in 1891 launched a new division in inorganic chemistry.[1] With the proof provided that alkali metals can react directly with base metals in liquid ammonia, a new class of materials was accessible in solution: ligand-free main group metal cluster anions.[2] In the 1930s systematic potentiometric titration experiments by *E. Zintl* gave rise to a very versatile main group chemistry of the heavier elements of the p-block elements.[3–5] The electron(s) of the less electronegative element are transferred to the more electronegative one under the formation of polyanionic salts, which are commonly known as Zintl phases.[5–8] When prepared via classical solid-state synthesis, most of these salt-like materials conversely are soluble in liquid ammonia. In the past, an impressive number of solvate structures containing homoatomic polyanions of group 14 to group 16 elements were prepared in non-aqueous solutions, which proves their stability as isolated entities in a wide range of different chemical surroundings.[9–11]

Tetrahedra are the smallest possible three-dimensional clusters. They can be found in the Zintl phases A_4Tt_4 (*A* = Na–Cs, *Tt* = Si–Pb) or in $A_{12}Tt_{17}$ together with a nine-vertex cluster, both of which can be obtained by a solid-state reaction from the elements.[9,12] The $[Tt_4]^{4-}$ clusters are well studied and crystal structures with isolated tetrahedra from solutions are known, as well as binary four-vertex clusters, which mix not only different group 14 elements but can also contain group 13 or 15 elements.[11,13] According to the pseudo-element concept,[7] those clusters can be related to the elemental structure of white phosphorus, which also holds true for the triel tetrahedra $[Tr_4]^{8-}$ (*Tr* = Al–Tl). Indeed, these clusters are known in solid-state for a small number of binary and ternary materials.[7,14, 15] Mixtures of alkaline earth metals and Al, Ga, or In yielded the compounds Ba_8Ga_7, Sr_8Ga_7, Sr_8Al_7,[16] compounds in the $Ca_{11}Ga_7$ type structure, which contain $[Tr_4]^{8-}$.[17] Also, a compound with group 14 germanium and group 13 aluminum, $Sr_{14}[Al_4]_2[Ge]_3$, is known to incorporate $[Al_4]^{8-}$ clusters.[18] Concentrating only on alkali metal thallides, only two phases with isolated tetrahedra are reported. Firstly, $Na_{23}K_9Tl_{15.3}$ by *Dong* and *Corbett* contains $[Tl_4]^{8-}$ clusters beside $[Tl_5]^{7-}$ trigonal bipyramids, $[Tl_3]^{7-}$ chains, and $[Tl]^{5-}$ ions.[19] Secondly, the Zintl phase Na_2Tl was reported in 1967 by *Hansen* and *Smith* and is the only known thallide, which features isolated $[Tr_4]^{8-}$ tetrahedra as the exclusive anionic moiety.[20,21] The observation of this thallide composition has been limited to the small alkali metal sodium so far. For the heavier congeners of the alkali metals, no 2:1 phase has been reported yet.

The colored liquid ammonia solutions, like the ones first observed by *Joannis* in 1891, demonstrated the accessibility of ligand-free main group metal clusters of group 14 or group 15

[a] *V. F. Schwinghammer, M. Janesch, Prof. Dr. N. Korber, Dr. S. Gärtner*
Department of Inorganic Chemistry
University of Regensburg
93040 Regensburg
E-mail: Stefanie.Gaertner@ur.de
[b] *Dr. S. Gärtner*
Central Analytics
University of Regensburg
93040 Regensburg

Supporting information for this article is available on the WWW under https://doi.org/10.1002/zaac.202200332

© 2022 The Authors. Zeitschrift für anorganische und allgemeine Chemie published by Wiley-VCH GmbH. This is an open access article under the terms of the Creative Commons Attribution Non-Commercial NoDerivs License, which permits use and distribution in any medium, provided the original work is properly cited, the use is non-commercial and no modifications or adaptations are made.

15213749, 2022, 24, Downloaded from https://onlinelibrary.wiley.com/doi/10.1002/zaac.202200332 by Universitaet Regensburg, Wiley Online Library on [19/12/2022]. See the Terms and Conditions (https://onlinelibrary.wiley.com/terms-and-conditions) on Wiley Online Library for rules of use; OA articles are governed by the applicable Creative Commons License

15213749, 2022, 24, Downloaded from https://onlinelibrary.wiley.com/doi/10.1002/zaac.202200332 by Universitaet Regensburg, Wiley Online Library on [19/12/2022]. See the Terms and Conditions (https://onlinelibrary.wiley.com/terms-and-conditions) on Wiley Online Library for rules of use; OA articles are governed by the applicable Creative Commons License

in solution. In contrast, when applied to group 13 elements, the liquid ammonia route only yields insoluble materials.[4] The first and most popular representative is sodium thallide, which also was the first fully characterized Zintl phase.[22] As NaTl includes a three-dimensional diamond-like sub-lattice of thallium atoms, the insolubility of this material is not surprising. Compared to tetrelides and pentelides of the alkali metals, thallides are special due to the high amount of group 1 elements possible in the compositions. A_xTl_y (A = Li–Cs) materials form three-dimensional networks, two-dimensional layers, or isolated clusters, dependent on the amount and nature of alkali metal involved. Only in some cases, they can be described as Zintl compounds. When isolated clusters are present in the respective solid state material, this also means a high content of alkali metal due to the high charge of the anionic moiety.[23]

We here report on the preparation and characterization of Na_7RbTl_4, which represents the first ternary, and contemporaneously the only second thallide, which exclusively contains isolated, tetrahedral $[Tl_4]^{8-}$ units. Additionally, the solubility of Na_2Tl and Na_7RbTl_4 in liquid ammonia was investigated.

Results and Discussion

X-Ray Structure Analysis of Single Crystals of Na_7RbTl_4 and Redetermination of Na_2Tl at 123 K

The new ternary compound Na_7RbTl_4 was found in experiments starting from the compositions $Na_4RbTl_{2.5}$ as well as Na_7RbTl_4. The bulk material was characterized by powder diffraction analysis and was obtained as a nearly pure phase with only a small number of non-indexed reflections of unknown origin (see powder diffraction patterns in SI). From this bulk phase, different single crystals were selected, which all suggested tetragonal symmetry according to the diffraction pattern. Despite all efforts, no structure solution and refinement in different tetragonal space groups succeeded. Chemical twinning is a common phenomenon in ternary Zintl phases.[24] In the here discussed phase, mixing of the alkali metals results in crystallographic twinning. Symmetry reduction to the orthorhombic crystal system finally yielded a structure model in the space group *Pbam* (No. 55) when pseudo-merohedral twinning was considered (twin law (0, 1, 0, −1, 0, 0, 0, 0, 1), BASF: 0.3437(5)). This explains the pretended tetragonal symmetry, as the twin law simulates a fourfold axis along *c*. In several measured crystals, the proportions of the twin components are variable and far from 50%, which proves the absence of proper fourfold symmetry. The crystallographic data, atomic coordinates, and interatomic distances are shown in Tables 1, 2, and 3.

Table 1. Crystallographic data and structure refinement parameters for Na_7RbTl_4.

Empirical Sum Formular	Na_7RbTl_4
CSD number	2208674
Formula weight	1063.88
Temperature/K	123
Crystal system	orthorhombic
Space group	*Pbam*
a/Å	16.3584(4)
b/Å	= a
c/Å	11.3345(3)
Volume/Å^3	3033.04(14)
Z	8
ρ_{calc}/(g/cm^3)	4.660
μ/mm^{-1}	24.713
F(000)	3504.0
Crystal size/mm^3	0.098 × 0.08 × 0.067
Radiation λ/Å	AgKα (0.56087)
2θ range for data collection/°	4.846 to 55.73
Index ranges	$-27 \le h, k \le 27$, $-18 \le l \le 18$
Collected/Independent reflections	79006/7639
Data/restraints/parameters	7639/0/126
Goodness-of-fit on F^2	1.086
R_{int}	0.0588
Final R indexes [$I \ge 2\sigma(I)$]	R_1 = 0.0231, wR_2 = 0.0393
Final R indexes [all data]	R_1 = 0.0282, wR_2 = 0.0402
Largest diff. peak/hole/eÅ^{-3}	1.73/−1.95

Comparison of Na_2Tl and Na_7RbTl_4

Anionic Substructures

As in Na_2Tl, which was reported by *Hansen* and *Smith*, the crystal structure of Na_7RbTl_4 contains tetrathallide tetrahedra as the anionic structural entity.[20] The asymmetric unit consists of six thallium, two rubidium, and ten sodium atomic sites. The observed two symmetry inequivalent tetrahedra (Tl1, Tl5, Tl6) and (Tl2, Tl3, Tl4) are formed by symmetry generated Tl positions of Tl1 and Tl2 (Wyckoff position 8*i*) and completed by the thallium positions Tl3–Tl6 (Wyckoff positions 4*g*/4*h*). Each thallium tetrahedron is coordinated by 16 sodium atoms (d(Na–Tl)≤3.6 Å) and five rubidium atoms (d(Rb–Tl)≤4.3 Å) (Figure 1, Tab.3).

Hansen and *Smith* reported for the tetrahedron in Na_2Tl a maximum deviation of 2° from the ideal 60° angle of the faces.[20] In the new compound Na_7RbTl_4, there are two different tetrahedra present, from which tetrahedron 2 (Tl2, Tl3, Tl4) shows also a 2° deviation, while tetrahedron 1 (Tl1, Tl5, Tl6) has a maximal deviation of 6°. The Tl–Tl distances within the altogether three Tl_4 clusters (one in Na_2Tl and two in Na_7RbTl_4) differ significantly referring to one short and one long edge (see Table 3). In the first coordination sphere, the Tl_4 tetrahedra are coordinated by four face capping sodium atoms (cluster 1: Na3, Na7, Na8; cluster 2: Na1, Na5, Na6), so that a binary tetrahedral star is formed.[25] The remaining sodium atoms in the coordination sphere are found to be exo coordinating or

 © 2022 The Authors. Zeitschrift für anorganische und allgemeine Chemie published by Wiley-VCH GmbH

15213749, 2022, 24, Downloaded from https://onlinelibrary.wiley.com/doi/10.1002/zaac.202200332 by Universitaet Regensburg, Wiley Online Library on [19/12/2022]. See the Terms and Conditions (https://onlinelibrary.wiley.com/terms-and-conditions) on Wiley Online Library for rules of use; OA articles are governed by the applicable Creative Commons License

Table 2. Standardised fractional atomic coordinates and equivalent isotropic displacement parameters for Na_7RbTl_4. U_{eq} is defined as 1/3 of the trace of the orthogonalized U_{ij} tensor.

Atom	x	y	z	Wyckoff position	$U_{eq}/Å^2$
Tl1	0.33568(2)	0.00890(2)	0.14415(2)	8*i*	0.01110(4)
Tl2	0.48921(2)	0.33762(29	0.35529(2)	8*i*	0.01119(4)
Tl3	0.00495(2)	0.3376(2)	0.5	4*h*	0.01142(5)
Tl4	0.14902(2)	0.20097(2)	0.5	4*h*	0.01237(5)
Tl5	0.16672(2)	0.00608(2)	0	4*g*	0.01186(5)
Tl6	0.19449(2)	0.34803(2)	0	4*g*	0.01273(6)
Rb1	0.31963(5)	0.00535(5)	0.5	4*h*	0.02152(17)
Rb2	0.01534(5)	0.18283(5)	0	4*g*	0.02283(16)
Na1	0.12163(14)	0.31875(14)	0.2684(2)	8*i*	0.0173(4)
Na2	0.17848(14)	0.11049(15)	0.2518(2)	8*i*	0.0203(5)
Na3	0.32260(14)	0.38069(14)	0.2094(2)	8*i*	0.0202(5)
Na4	0.39578(15)	0.17668(14)	0.2603(2)	8*i*	0.0209(5)
Na5	0.0906(2)	0.00324(17)	0.5	4*h*	0.0194(8)
Na6	0.32422(19)	0.2813(2)	0.5	4*h*	0.0193(7)
Na7	0.00552(18)	0.4093(2)	0	4*g*	0.0200(8)
Na8	0.28013(19)	0.17659(18)	0	4*g*	0.0163(6)
Na9	0	0.5	0.3047(4)	4*f*	0.0172(8)
Na10	0	0	0.1888(4)	4*e*	0.0224(8)

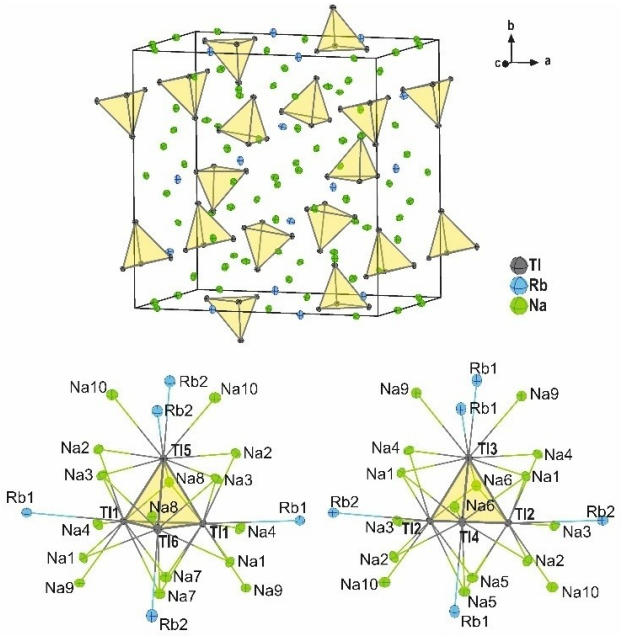

Figure 1. Top: Unit cell of Na_7RbTl_4 with Tl_4^{8-} tetrahedra marked in yellow. Bottom: Coordination sphere of both Tl-tetrahedra.

edge capping (Figure 1). The significant difference between Na_2Tl and Na_7RbTl_4 is of course caused by the rubidium atoms, which widen the structure and reduce the number of the tetrahedra coordinating atoms from 23 in Na_2Tl to 21 in the ternary phase.

Alkali Metal Coordinations

The symmetry inequivalent rubidium atoms Rb1 (Wyckoff position *4h*) and Rb2 (Wyckoff position *4g*) in Na_7RbTl_4 show contacts to altogether 18 neighboring atoms (5x Tl, 13x Na). The five thallium atoms all belong to different tetrahedral entities, resulting in a square pyramidal arrangement of Tl_4 clusters around Rb. While the coordination number (CN) in Na_2Tl varies between 12 and 14, Na_7RbTl_4 shows CN values of 11, 12, 14, and 18. In Na_7RbTl_4, the ten symmetry inequivalent sodium atoms show contacts to two to four Tl_4 units. The coordination of sodium can be divided and grouped by the coordination numbers and the type of coordination (Figure 2). Na9 (Wyckoff position 4*f*) and Na10 (Wyckoff position 4*e*) coordinate on four vertices of unique tetrahedral entities. There are also six additional Na and two Rb in the first coordination sphere. The next group consists of Na3 (Wyckoff position 8*i*), Na6 (Wyckoff position 4*h*), and Na8 (Wyckoff position 4*g*). Here, one face-capping tetrahedron is present, and a second tetrahedron coordinates via its vertex. Furthermore, there are five more sodium and two rubidium atoms.

Na5 (Wyckoff position 4*h*) and Na7 (Wyckoff position 4*g*) each coordinate to a tetrahedral face and one edge of Tl_4 clusters. Additionally, they are surrounded by one Rb and six or eight Na atoms. Na1 (Wyckoff position 8*i*), Na2 (Wyckoff position 8*i*), and Na4 (Wyckoff position 8*i*) have a coordination number of 12 including two rubidium atoms. Only the number and type of coordination to the thallium clusters differ and affect the number of sodium atoms. While every of these three alkali metal positions coordinates μ_2 to a tetrahedral edge, there is one further coordination to a tetrahedron (Na4: μ_1 vertex, Na2: μ_2 edge, Na1: μ_3 face). In general, a direct comparison between the alkali metal coordination of Na_2Tl and Na_7RbTl_4 is not possible, but the CN and the type of coordination of the alkali metal atoms towards the Tl_4 clusters can be checked for

 © 2022 The Authors. Zeitschrift für anorganische und allgemeine Chemie published by Wiley-VCH GmbH

15213749, 2022, 24, Downloaded from https://onlinelibrary.wiley.com/doi/10.1002/zaac.202200332 by Universitaet Regensburg, Wiley Online Library on [19/12/2022]. See the Terms and Conditions (https://onlinelibrary.wiley.com/terms-and-conditions) on Wiley Online Library for rules of use; OA articles are governed by the applicable Creative Commons License

Table 3. Interatomic distances (d(Tl–Tl) < 3.3 Å, d(Tl–Na) < 3.6 Å, d(Tl–Rb) < 4.3 Å, d(Na–Rb) < 4.6 Å, d(Na–Na) < 4.0 Å).

Neighbor	d/Å	Neighbor	d/Å	Neighbor	d/Å
Tl1		Tl2		Tl3	
Tl1	3.2677(5)	Tl2	3.2803(4)	Tl4	3.2143(4)
Tl5	3.2110(3)	Tl3	3.2698(3)	Rb1	4.0057(9)
Tl6	3.1366(3)	Tl4	3.1500(3)	Rb1	4.0046(9)
Rb1	4.0423(2)	Rb2	4.0635(3)	Na1	3.256(2)
Na1	3.485(2)	Na1	3.494(2)	Na1	3.256(2)
Na2	3.296(2)	Na2	3.418(2)	Na4	3.256(3)
Na3	3.413(2)	Na3	3.265(2)	Na4	3.256(3)
Na4	3.199(2)	Na4	3.229(2)	Na6	3.512(3)
Na7	3.475(3)	Na5	3.425(3)	Na9	3.497(3)
Na7	3.490(3)	Na5	3.495(3)	Na9	3.497(3)
Na8	3.320(3)	Na6	3.290(3)		
Na9	3.250(2)	Na10	3.263(3)		
Tl4		Tl5		Tl6	
Rb1	4.2461(9)	Tl6	3.4408(4)	Rb2	3.9864(9)
Na1	3.287(2)	Rb2	3.8067(9)	Na1	3.302(2)
Na1	3.287(2)	Rb2[1]	4.2919(9)	Na1	3.302(2)
Na2	3.215(2)	Na2	3.332(2)	Na3	3.211(2)
Na2	3.215(2)	Na2	3.332(2)	Na3	3.211(2)
Na5	3.373(3)	Na3	3.142(2)	Na7	3.249(3)
Na6	3.153(3)	Na3[2]	3.142(2)	Na8	3.135(3)
		Na8	3.350(3)		
		Na10	3.468(3)		
		Na10	3.468(3)		
Rb1		Rb2		Na1	
Na1	4.139(2)	Na1	4.150(3)	Na2	3.536(3)
Na1	4.139(2)	Na1	4.150(3)	Na3	3.504(3)
Na2	4.025(2)	Na2	4.083(2)	Na4	3.696(4)
Na2	4.025(2)	Na2	4.083(2)	Na7	3.880(3)
Na3	4.518(3)	Na3	4.081(3)	Na9	3.594(2)
Na3	4.518(3)	Na3	4.081(3)		
Na4	4.097(3)	Na4	4.220(2)		
Na4	4.097(3)	Na4	4.220(2)		
Na5	3.747(4)	Na7	3.707(4)		
Na6	4.355(3)	Na8	4.332(3)		
Na6	4.514(3)	Na8	4.482(3)		
Na9	3.690(3)	Na10	3.686(3)		
Na9	3.690(3)	Na10	3.686(3)		
Na2		Na3		Na4	
Na3	3.790(4)	Na4	3.592(3)	Na6	3.417(3)
Na4	3.717(3)	Na6	3.673(3)	Na7	3.729(3)
Na5	3.614(3)	Na10	3.505(2)	Na8	3.505(3)
Na8	3.475(3)			Na9	3.393(2)
Na10	3.507(3)				
Na5		Na7			
Na5	2.965(8)	Na7	2.974(8)		
Na6	3.890(5)	Na8	3.945(4)		
Na10	3.826(5)	Na9	3.760(4)		
Na10	3.826(5)	Na9	3.760(4)		

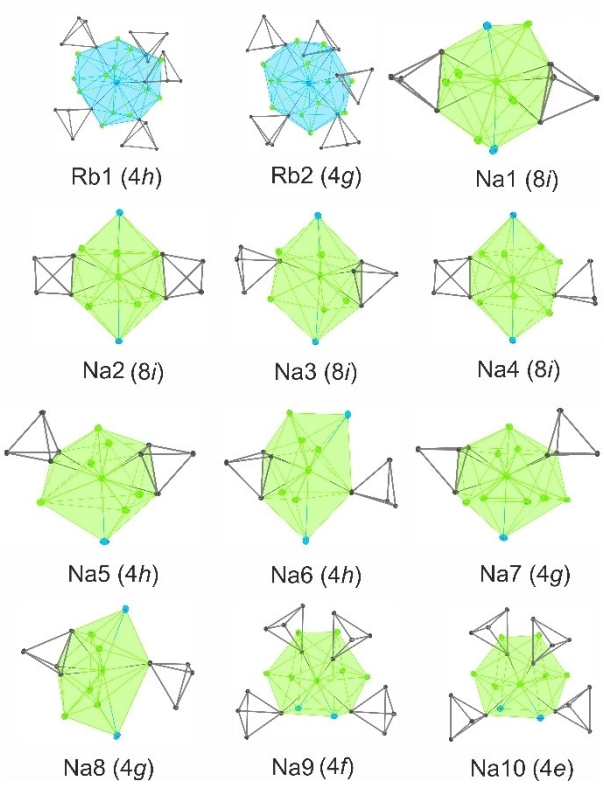

Figure 2. Coordination spheres of the symmetrically inequivalent alkali metal positions in Na_7RbTl_4.

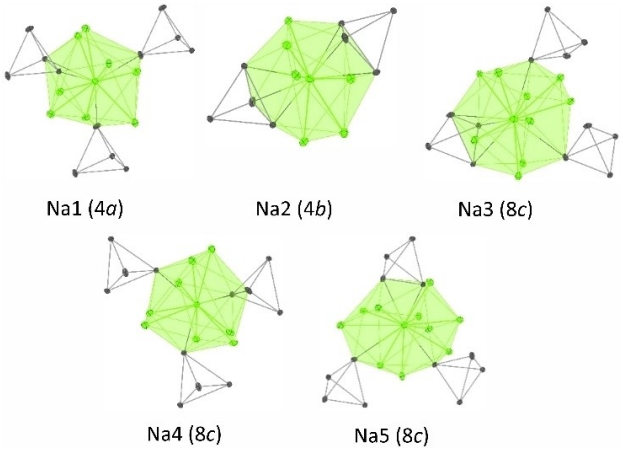

Figure 3. Coordination spheres of the five symmetrically inequivalent sodium atoms in Na_2Tl.

similarity. In Na_2Tl very similar arrangements around the sodium atoms are found (Figure 3). The major discrepancy is observed for Na2 (Wyckoff position *4h*) in Na_2Tl, which coordinates μ_3 to the faces of two different Tl_4 anions. This kind of rather dense "sandwich-like" coordination could not be observed in the new phase Na_7RbTl_4.

 © 2022 The Authors. Zeitschrift für anorganische und allgemeine Chemie published by Wiley-VCH GmbH

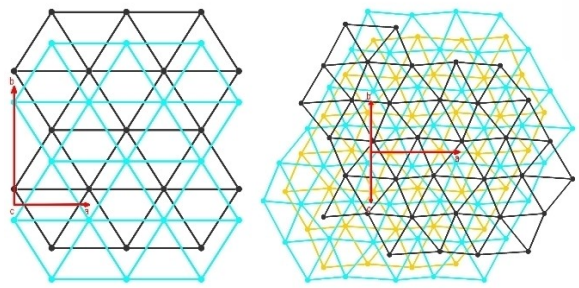

Figure 4. Section of the thallium part of the crystal structures of Na_2Tl (left) and Na_7RbTl_4 (right) where Tl_4 clusters are replaced by their centers (as balls with fixed radii) to illustrate the repeating layers in the sequence AB for Na_2Tl and ABC for Na_7RbTl_4. The red arrows represent the unit cell edges.

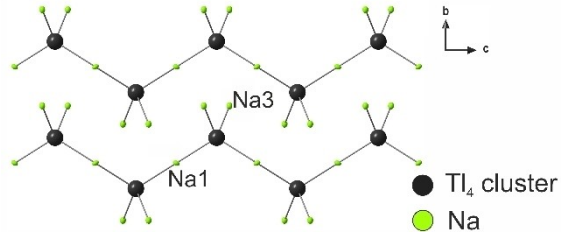

Figure 5. Zig-zag chains in Na_2Tl formed by vertex connected Na_4Tl_4 tetrahedral star units along the crystallographic *c*-axis. The Tl_4 clusters are represented by their centers as black balls with fixed radii.

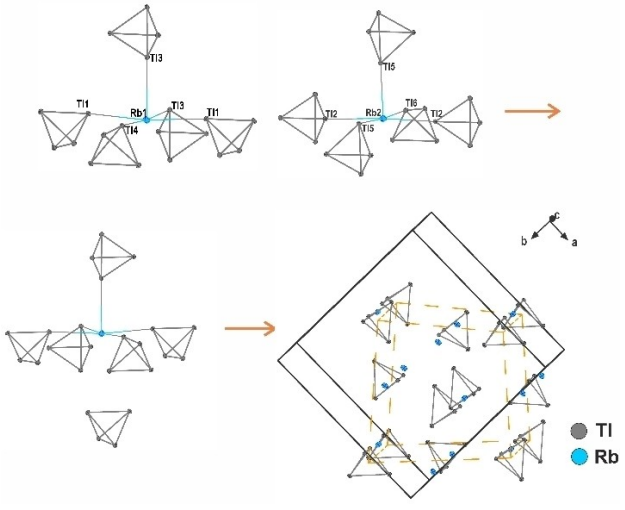

Figure 6. Rb1 and Rb2 with their five Tl_4 clusters in the first coordination sphere (d(Rb–Tl) < 4.6 Å) (up), octahedral environment of the rubidium atom after the extended distance range (d(Rb–Tl) - < 6.1 Å (down, left) and the NaCl structure-like arrangement of the thallium clusters and rubidium in Na_7RbTl_4 with the unit cell edges from Na_7RbTl_4 marked black and from the distorted NaCl structure-like arrangement marked orange (down).

Three-dimensional Arrangement

The tetrahedra in the crystal structures are arranged in layers perpendicular to [0 0 1] (Na_2Tl) and [0 1 1] (Na_7RbTl_4). In Figure 4, each tetrahedron is replaced by its center to visualize the three-dimensional arrangement in a more comprehensible way. The stacking sequence of the tetrahedral clusters of ABAB is observed for Na_2Tl and ABC for Na_7RbTl_4. This shows nicely that Na_2Tl can be derived from a hcp (hexagonal closed packing) of the Tl_4 subunits, which is in accordance with the observed space group symmetry $C222_1$ for Na_2Tl, a subgroup of $P6_3/mmc$ (hcp). In contrast, the stacking sequence ABCABC of the Tl_4 subunits in the new thallide is related to the cubic closed packing (ccp).

While in Na_2Tl Na_4Tl_4 tetrahedral star units are linked at one vertex and form zig-zag chains in the crystallographic *c* direction (Figure 5), in Na_7RbTl_4 five Tl_4 clusters are connected by one rubidium position, which coordinates μ_1 on every cluster vertex.

This $Rb(Tl_4)_5$ resembles a slightly distorted square pyramid (Figure 6). When considering the second coordination sphere of the Rb atoms (d(Rb–Tl)< 6.1 Å), a sixth tetrahedron was identified, resulting in a distorted octahedral environment for Rb.

Due to the fact that the rubidium atoms are located in the octahedral voids of the distorted ccp arrangement of the thallium clusters, Na_7RbTl_4 can be described as containing distorted NaCl type $[Rb(Tl_4)]^{7-}$-substructure, which presumably is the driving force for the formation of the observed structure. The sodium atoms fill up this arrangement resulting in an electroneutral Na_7RbTl_4 composition in agreement with an eightfold negatively charged $[Tl_4]^{8-}$ cluster. Experiments with the goal to realize the same type structure for cesium instead of rubidium have also been performed but did not succeed.

Calculations of the Electronic Structure

Initial theoretical calculations based on the crystal structures prove the semi-metallic character, hence support the ionic description of the considered materials. According to the (8-*N*) rule,[6] $[Tl_4]^{8-}$ is an electron-precise cluster. Each edge of the tetrahedron corresponds to an electron precise 2center-2electron bond. For Na_2Tl and its heavier homologue Na_7RbTl_4, the 6*p* orbitals are considered to participate in the bonding.[20] The sodium atoms donate their electrons in these orbitals, which leads to a closed shell configuration. According to this ionic description, both compounds exhibit a pseudo band gap. The tDOS (Figure 7) reveals that the Fermi level E_F falls into a narrow gap for both compounds.[6,26]

Dissolving Thallides in Liquid Ammonia

For most group 14 solid state phases combining alkali metals with $[Tt_4]^{4-}$ clusters, solubility in liquid ammonia has been observed.[9] Although of course the higher charges of the $[Tr_4]^{8-}$

 © 2022 The Authors. Zeitschrift für anorganische und allgemeine Chemie published by Wiley-VCH GmbH

15213749, 2022, 24, Downloaded from https://onlinelibrary.wiley.com/doi/10.1002/zaac.202200332 by Universitaet Regensburg, Wiley Online Library on [19/12/2022]. See the Terms and Conditions (https://onlinelibrary.wiley.com/terms-and-conditions) on Wiley Online Library for rules of use; OA articles are governed by the applicable Creative Commons License

15213749, 2022, 24, Downloaded from https://onlinelibrary.wiley.com/doi/10.1002/zaac.202200332 by Universitaet Regensburg, Wiley Online Library on [19/12/2022]. See the Terms and Conditions (https://onlinelibrary.wiley.com/terms-and-conditions) on Wiley Online Library for rules of use; OA articles are governed by the applicable Creative Commons License

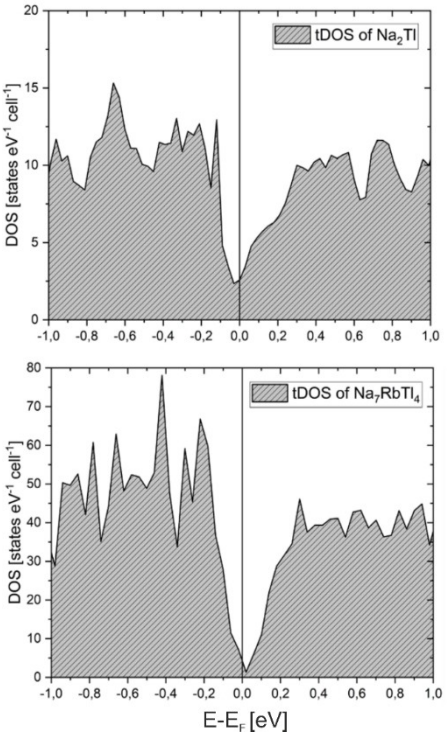

Figure 7. tDOS of Na_2Tl and Na_7RbTl_4 show pseudo band gap around the Fermi level. Both components are classical semi metals.

suggest insolubility, the salt-like character encouraged us to investigate this experimentally. Homoatomic polyanions in solution are known to be very sensitive towards protonation.[27] This in return is the first step of degradation as protonation also means oxidation for less electronegative main group metals. The best solvent for highly charged homoatomic polyanions is liquid ammonia, due to its highly polar but less protic character. For this reason, solubility tests were carried out with Na_2Tl and Na_7RbTl_4. The compounds were weighted into a three-times-baked-out reaction vessel using a glove box. Subsequently, liquid ammonia was condensed at 195 K using the standard Schlenk-technique.

In general, there are three different possible observations that can be made while condensing ammonia onto a product of the solid-state reaction. Firstly, no change in color can be observed, which indicates insolubility. Secondly, a blue solution means solvated electrons.[26] Thirdly, a change in color different from blue is possible, pointing to dissolved stable main group cluster anions. For Na_2Tl and Na_7RbTl_4 dark blue coloring of the solutions was observed (Figure 8), which indicates the transfer of electrons into the solvent and thus the degradation of the saltlike compound.

After one month of storage at 233 K, the solution was clear and colorless with a residue. The residue was characterized by X-ray powder diffraction experiments after the evaporation of ammonia. Alkali metal amide and elemental thallium were identified as products (see SI). This experiment demonstrated that, while $[Tl_4]^{8-}$ clusters are not transferable in solution, the

Figure 8. Solubility test of Na_2Tl and Na_7RbTl_4 shows a dark blue solution (left) with the colorless solution with residue after storing for one month (middle) and residue after evaporation of the liquid ammonia (right).

compounds Na_2Tl or Na_7RbTl_4 are not insoluble, and that dissolution causes fast decomposition. Future experiments of less charged thallide cluster compounds will show if this is a common feature for this class of materials or if also insolubility or even perhaps somewhat stable solutions are possible.

Conclusions

We here report on the synthesis and characterization of the ternary compound Na_7RbTl_4. Single crystal x-ray structure analysis reveals the presence of $[Tl_4]^{8-}$ tetrahedra, which are known from binary Na_2Tl. Due to the insertion of the larger alkali metal rubidium, the tetrahedra themselves show a greater degree of distortion. As a further consequence of rubidium being involved, the three-dimensional arrangement of $[Tl_4]^{8-}$ anions changes from a distorted hexagonal closed packed (hcp) arrangement in Na_2Tl to a distorted cubic closed packed (ccp) packing of the tetrahedra in Na_7RbTl_4. The large Rb cations are located in the octahedral voids of the ccp, which results in a NaCl-type subunit for $[Rb(Tl_4)]^{7-}$.

Theoretical calculations using *FPLO21*[28] for Na_2Tl as well as for Na_7RbTl_4 showed a pseudo band gap at E_F and suggest classical semi-metallic character of the latter.

Solvation tests in liquid ammonia proved for both compounds decomposition in solution by forming alkali metal amide and elemental thallium.

Experimental Section

Materials: Sodium (purity 99%, under mineral oil, Merck/Sigma-Aldrich, Darmstadt) was segregated for purification. Rubidium was obtained by reduction of RbCl with elemental calcium[29] and afterward purified through two times distillation. Thallium drops (purity 99.99%, ABCR) were used without further purification and were stored under an inert gas atmosphere.

Preparation: The elements were placed in tantalum ampoules and sealed under an argon atmosphere. The sealed ampoules were placed in quartz glass tubes (QSIL GmbH, Ilmenau, Germany), which were also sealed under an argon atmosphere. For both compositions, the same temperature program was used: heating up from room temperature to 673.15 K with a heating range of 100 K per hour, holding for 4 hours, cooling down to 473.15 K, holding again for 1 hour, and then cooling down to room temperature with a cooling rate of 3 K per hour. The products received are very

 © 2022 The Authors. Zeitschrift für anorganische und allgemeine Chemie published by Wiley-VCH GmbH

15213749, 2022, 24, Downloaded from https://onlinelibrary.wiley.com/doi/10.1002/zaac.202200332 by Universitaet Regensburg, Wiley Online Library on [19/12/2022]. See the Terms and Conditions (https://onlinelibrary.wiley.com/terms-and-conditions) on Wiley Online Library for rules of use; OA articles are governed by the applicable Creative Commons License

sensitive to moisture and oxygen. Therefore, they were stored in a glove box (Labmaster 130 G, Fa. M. Braun, Garching, Germany).

X-Ray Single Crystal Analysis: A small number of crystals was transferred into dried mineral oil. A suitable crystal was selected and mounted on a Rigaku SuperNova diffractometer (Rigaku Polska sp. Z. o. o. UI, Wroclaw, Poland) (X-ray: Ag microfocus, AtlasS2 detector) using MiTeGen loops. All data were collected at 123 K.

CrysAlisPro (Version 41_64.93a) was used for data collection and data reduction.[30] For the structure solution, *ShelXT* was used and the subsequent data refinement was carried out with *ShelXL*.[31] *Olex*^{2} was taken for visualization purposes and the software *Diamond4* was chosen for the representation of the crystal structure.[31] All atoms are depicted as ellipsoids with a 50% probability level.

Crystallographic data for the compounds have been deposited in the Cambridge Crystallographic Data Center, CCDC, 12 Union Road Cambridge CB21EZ, UK. Copies of the data can be obtained free of charge under the depository number CCDC-2208674 (Na_7RbTl_4) and CCDC-2208786 (Na_2Tl redetermined at 123 K) (Fay: +44-1223-336-033, E-Mail: deposit@ccdc.cam.ac.uk, http://www.ccdc.cam.ac.uk).

Powder Diffraction Studies: Powder diffraction samples were prepared in sealed capillaries (∅ 0.3 mm, WJM-Glas-Müller GmbH, Berlin, Germany). The data collection was carried out on a STOE Stadi P diffractometer (STOE, Darmstadt, Germany) (Monochromatic MoKα1 radiation, $\lambda = 0.70926$ Å) equipped with a Dectris Mythen 1 K detector. For visualization and indexation, the software WinXPOW was used.[33]

DFT Calculations: For the theoretical calculations the program *FPLO21*[28] was used, which is based on the *full-potential non-orthogonal local orbital minimum-basis* within the *generalized gradient approximation* (GGA) for full-relativistic mode. It turned out that for the heavy atom thallium a full-relativistic approach is necessary because a neglection of the spin-orbit coupling (SOC) leads to different results than using the full-relativistic approach.[15] The exchange correlation was assumed in the form proposed by *Perdew*, *Burke* and *Ernzerhof* (PBE).[34] For the calculation of the density of states (DOS) a modular grid for the reciprocal space of 2000 *k*-points was sufficient. For the calculation of the band structure (see SI) 6x6x6 *k*-points were used. As convergence criterion a change of the total energy ($\Delta E_{tot} \leq 10^{-6}$ Hartree) was applied. For the visualization of the band structure, the program *xfbp*[28] was used and the DOS was plotted with *Origin2022* (version 9.9.0.225).[35]

Acknowledgements

The authors thank Dr. Pielnhofer for the support of the theoretical calculations, Prof. Röhr for very valuable discussions, and Florian Wegner (AK Prof. Pfitzner) for powder diffraction experiments. This research was funded by the German Science Foundation (DFG) (GA 2504/1-1). Open Access funding enabled and organized by Projekt DEAL.

Conflict of Interest

The authors declare no conflict of interest.

Data Availability Statement

The data that support the findings of this study are available in the supplementary material of this article.

Keywords: Thallium · Cluster · X-Ray Structure · Alkali Metals · Zintl · Single Crystals · Liquid Ammonia

[1] A. C. Joannis, *C. R. Hebd. Seances Acad. Sci.* **1891**, *113*, 795–798.
[2] a) C. A. Kraus, *J. Am. Chem. Soc.* **1907**, *29*, 1557–1571; b) C. A. Kraus, *J. Am. Chem. Soc.* **1922**, *44*, 1216–1239.
[3] a) E. Zintl, A. Harder, *Z. Phys. Chem.* **1931**, *A154*, 47–91; b) E. Zintl, H. Kaiser, *Z. Anorg. Allg. Chem.* **1933**, *211*, 113–131.
[4] E. Zintl, J. Goubeau, W. Dullenkopf, *Z. Phys. Chem.* **1931**, *154*, 1–46.
[5] E. Zintl, *Angew. Chem.* **1939**, *52*, 1–6.
[6] A. Kjekshus, *Acta Chem. Scand.* **1964**, *18*, 2379–2384.
[7] R. Nesper, *Z. Anorg. Allg. Chem.* **2014**, *640*, 2639–2648.
[8] A. M. Guloy, in *Inorganic Cemistry in Focus III*, Wiley-VCH Verlag GmbH & Co, Weinheim, Germany, **2006**.
[9] C. Liu, Z. M. Sun, *Coord. Chem. Rev.* **2019**, *382*, 32–56.
[10] a) Ed. T. F. Fässler, *Zintl Phases - Principles and recent developments, Vol. 139*, Springer, Berlin, Heidelberg, **2011**; b) S. Scharfe, F. Kraus, S. Stegmaier, A. Schier, T. F. Fässler, *Angew. Chem. Int. Ed.* **2011**, *50*, 3630–3670; *Angew. Chem.* **2011**, *123*, 3712–3754.
[11] F. Pan, L. Guggolz, S. Dehnen, *CCS* **2022**, *4*, 809–824.
[12] a) H. G. von Schnering, M. Schwarz, J. H. Chang, K. Peters, E. M. Peters, R. Nesper, *Z. Kristallogr.* **2005**, *220*, 525–527; b) T. Goebel, Y. Prots, F. Haarmann, *Z. Krist.-New Cryst. St.* **2008**, *223*, 187–188; c) J. Witte, H. G. von Schnering, *Z. Anorg. Allg. Chem.* **1964**, *327*, 260–273; d) M. Baitinger, K. Peters, M. Somer, W. Carrillo-Cabrera, Y. Grin, R. Kniep, H. G. von Schnering, *Z. Krist.-New Cryst. St.* **1999**, *214*, 455–456; e) M. Baitinger, Y. Grin, H. G. von Schnering, R. Kniep, *Z. Krist.-New Cryst. St.* **1999**, *214*, 457–458; f) R. Schäfer, W. Klemm, *Z. Anorg. Allg. Chem.* **1961**, *312*, 214–220; g) E. Hohmann, *Z. Anorg. Allg. Chem.* **1948**, *257*, 113–126; h) C. Hoch, M. Wendorff, C. Röhr, *J. Alloys Compd.* **2003**, *361*, 206–221; i) E. Busmann, *Z. Anorg. Allg. Chem.* **1961**, *313*, 90–106; j) T. Goebel, A. Ormeci, O. Pecher, F. Haarmann, *Z. Anorg. Allg. Chem.* **2012**, *638*, 1437–1445.
[13] a) K. Wiesler, K. Brandl, A. Fleischmann, N. Korber, *Z. Anorg. Allg. Chem.* **2009**, *635*, 508–512; b) W. Klein, C. B. Benda, T. Henneberg, B. J. L. Witzel, T. F. Fässler, *Z. Anorg. Allg. Chem.* **2021**, *647*, 2047–2054; c) C. Lorenz, S. Gärtner, N. Korber, *Crystals* **2018**, *8*, 276–276.
[14] a) F. Wang, G. J. Miller, *Inorg. Chem.* **2011**, *50*, 7625–7636; b) B. Lehmann, C. Röhr, *Z. Anorg. Allg. Chem.* **2022**, *648*, e202200204
[15] F. Wang, U. Wedig, D. Prasad, M. Jansen, *J. Am. Chem. Soc.* **2012**, *134*, 19884–19894.
[16] M. L. Fornasini, *Acta Crystallogr. Sect. C* **1983**, *39*, 943–946.
[17] a) M. L. Fornasini, F. Merlo, *Z. Kristallogr.* **1989**, *187*, 111–115; b) M. Wendorff, C. Röhr, *J. Alloy Compd* **2008**, *448*, 128–140.
[18] M. Wendorff, C. Röhr, *Z. Naturforsch. B* **2007**, *62*, 1227–1234.
[19] Z. C. Dong, J. D. Corbett, *Inorg. Chem.* **1996**, *35*, 3107–3112.
[20] D. A. Hansen, J. F. Smith, *Acta Crystallogr.* **1967**, *22*, 836–845.
[21] a) B. Li, J. D. Corbett, *Inorg. Chem.* **2006**, *45*, 2960–2964; b) S. C. Sevov, J. D. Corbett, *J. Solid State Chem.* **1993**, *103*, 114–130.
[22] E. Zintl, W. Dullenkopf, *Z. Phys. Chem.* **1932**, *B16*, 195–205.
[23] S. Gärtner, *Crystals* **2020**, *10*, 1013.
[24] F. Zürcher, S. Wengert, R. Nesper, *Inorg. Chem.* **1999**, *38*, 4567–4569.
[25] U. Häussermann, C. Svensson, S. Lidin, *J. Am. Chem. Soc.* **1998**, *120*, 3867–3880.

 © 2022 The Authors. Zeitschrift für anorganische und allgemeine Chemie published by Wiley-VCH GmbH

[26] L. M. Schoop, F. Pielnhofer, B. V. Lotsch, *Chem. Mater.* **2018**, *30*, 3155–3176.
[27] a) T. Henneberger, W. Klein, T. F. Fässler, *Z. Anorg. Allg. Chem.* **2018**, *644*, 1018–1027; b) C. Lorenz, F. Hastreiter, J. Hioe, N. Lokesh, S. Gärtner, N. Korber, R. M. Gschwind, *Angew. Chem. Int. Ed.* **2018**, *57*, 12956–12960; *Angew. Chem.* **2018**, *130*, 13138–13142; c) F. Hastreiter, C. Lorenz, J. Hioe, S. Gärtner, N. Lokesh, N. Korber, R. M. Gschwind, *Angew. Chem. Int. Ed.* **2019**, *58*, 3133–3137; *Angew. Chem.* **2019**, *131*, 3165–3169; d) V. Streitferdt, S. M. Tiefenthaler, I. G. Shenderovich, S. Gärtner, N. Korber, R. M. Gschwind, *Eur. J. Inorg. Chem.* **2021**, *2021*, 3684–3690.
[28] a) H. Eschrig, K. Koepernik, I. Chaplygin, *J. Solid State Chem.* **2003**, *176*, 482–495; b) K. Koepernik, H. Eschrig, *Phys. Rev. B* **1999**, *59*, 1743–1757. c) K. Lejaeghere, G. Bihlmayer, T. Bjorkman, P. Blaha, S. Blugel, V. Blum, D. Caliste, I.E. Castelli, S. J. Clark, A. Dal Corso, S. de Gironcoli, T. Deutsch, J. K. Dewhurst, I. Di Marco, C. Draxl, M. Dulak, O. Eriksson, J. A. Flores-Livas, K. F. Garrity, L. Genovese, P. Giannozzi, M. Giantomassi, S. Goedecker, X. Gonze, O. Granas, E. K. U. Gross, A. Gulans, F. Gygi, D. R. Hamann, P. J. Hasnip, N. A. W. Holzwarth, D. Iusan, D. B. Jochym, F. Jollet, D. Jones, G. Kresse, K. Koepernik, E. Kucukbenli, Y. O. Kvashnin, I. L. M. Locht, S. Lubeck, M. Marsman, N. Marzari, U. Nitzsche, L. Nordstrom, T. Ozaki, L. Paulatto, C. J. Pickard, W. Poelmans, M. I. J. Probert, K. Refson, M. Richter, G. M. Rignanese, S. Saha, M. Scheffler, M. Schlipf, K. Schwarz, S. Sharma, F. Tavazza, P. Thunstrom, A. Tkatchenko, M. Torrent, D. Vanderbilt, M. J. van Setten, V. Van Speybroeck, J. M. Wills, J. R. Yates, G. X. Zhang, S. Cottenier, *Science* **2016**, *351*, 6280; d) I. Opahle, K. Koepernik, H. Eschrig, *Phys. Rev. B* **1999**, *60*, 14035–14041.
[29] L. Hackspill, *Helv. Chim. Acta* **1928**, *11*, 1003–1026.
[30] CrysAlisPRO, Version 171.41.93a, Oxford Diffraction/Agilent Technologies UK Ltd, Yarnton, UK, **2020**.
[31] a) G. M. Sheldrick, *Acta Crystallogr. Sect. C* **2015**, *71*, 3–8; b) G. M. Sheldrick, *Acta Crystallogr. Sect. A* **2015**, *71*, 3–8.
[32] a) O. V. Dolomanov, L. J. Bourhis, R. J. Gildea, J. A. K. Howard, H. Puschmann, *J. Appl. Crystallogr.* **2009**, *42*, 339–341; b) K. Brandenburg, Diamond, Version 4.6.8, Crystal Impact GbR, Bonn, **2021**.
[33] WinXPOW, Version 3.4.6, STOE & Cie GmbH, Darmstadt, **2016**.
[34] J. P. Perdew, K. Burke, M. Ernzerhof, *Phy. Rev. Lett.* **1996**, *77*, 3865–3868.
[35] Origin(Pro), Version 9.9.0.225, OriginLab Cooperation, Northampton, MA, USA, **2021**.

Manuscript received: October 10, 2022
Revised manuscript received: November 23, 2022
Accepted manuscript online: December 1, 2022

 © 2022 The Authors. Zeitschrift für anorganische und allgemeine Chemie published by Wiley-VCH GmbH

15213749, 2022, 24, Downloaded from https://onlinelibrary.wiley.com/doi/10.1002/zaac.202200332 by Universitaet Regensburg, Wiley Online Library on [19/12/2022]. See the Terms and Conditions (https://onlinelibrary.wiley.com/terms-and-conditions) on Wiley Online Library for rules of use; OA articles are governed by the applicable Creative Commons License